

Characteristic of In Situ Stress and Its Control on the Coalbed Methane Reservoir Permeability in the Eastern Margin of the Ordos Basin, China

Junlong Zhao^{1,2} · Dazhen Tang^{1,2} · Hao Xu^{1,2} · Yong Li³ · Song Li^{1,2} · Shu Tao^{1,2} · Wenji Lin⁴ · Zhenxing Liu⁵

Received: 9 September 2015 / Accepted: 20 March 2016 / Published online: 5 May 2016
© Springer-Verlag Wien 2016

Abstract Coalbed methane (CBM) development faces many challenges, among which in situ stress and permeability are two of the most important and fundamental factors. Knowledge of the characteristics of these factors is crucial to CBM exploration and development. Based on measured injection/falloff and in situ stress well test data of 55 CBM wells in the eastern margin of the Ordos Basin, correlations between parameters including initial reservoir pressure, in situ stress, lateral stress coefficient, well test permeability, and burial depth were determined. The distribution of in situ stress was analyzed systematically and its influence on permeability was also addressed. The results indicate that the maximum horizontal principal stress (σ_H 10.13–37.84 MPa, average 22.50 MPa), minimum horizontal principal stress (σ_h 6.98–26.88 MPa, average 15.04 MPa) and vertical stress (σ_v 12.30–35.72 MPa, average 22.48 MPa) all have positive correlations with coal burial depth. Stress ratios (σ_H/σ_h , σ_H/σ_v , and σ_h/σ_v) and lateral stress coefficient slowly

attenuated with depth. With increase of horizontal principal stresses, coal reservoir permeability (0.01–3.33 mD, average 0.65 mD) decreases. The permeability variation is basically consistent with change of stress state at a certain burial depth, the essence of which is the deformation and destruction of coal pore structures under the action of stresses. Three types of stress fields exist in the area: in the shallow coal seam at burial depths <700 m, the horizontal principal stress is dominant, revealing a strike slip regime ($\sigma_H > \sigma_v > \sigma_h$), with average permeability 0.89 mD; from 700 to 1000 m depths, there is a stress transition zone ($\sigma_H \approx \sigma_v > \sigma_h$) with average permeability 0.73 mD; in the deep coal seam with burial depths >1000 m, the vertical principal stress is dominant, demonstrating a normal stress regime ($\sigma_v > \sigma_H > \sigma_h$) with average permeability 0.11 mD.

Keywords In situ stress · Permeability · Burial depth · CBM · Coal reservoir

✉ Dazhen Tang
tang@cugb.edu.cn

Junlong Zhao
zhao739264823@126.com

Hao Xu
xuhao600@163.com

Yong Li
cugbliyong@gmail.com

Song Li
lisong85@126.com

Shu Tao
peach888@163.com

Wenji Lin
linwj@nccbm.com.cn

¹ School of Energy Resources, China University of Geosciences (Beijing), Beijing 100083, People's Republic of China

² Coal Reservoir Laboratory of National Engineering Research Center of Coalbed Methane Development and Utilization, Beijing 100083, People's Republic of China

³ College of Geoscience and Surveying Engineering, China University of Mining and Technology (Beijing), Beijing 100083, People's Republic of China

⁴ China United Coalbed Methane National Engineering Research Center Co., Ltd, Beijing 100095, People's Republic of China

⁵ Exploration and Development Research Institute of Huabei Oilfield Company, Renqiu 062552, People's Republic of China

List of Symbols

α	Coefficient depended on the principal stress type
a	Undetermined coefficient
b	Undetermined coefficient
CBM	Coalbed methane
H	Burial depth
ISIP	Instantaneous shut-in pressure
k	Permeability of a given stress condition
k_0	Permeability of the initial stress condition
p	Pressure
p_0	Rock pore pressure (initial reservoir pressure)
p_c	Closing pressure
p_f	Fracturing pressure
p_i	Injection pressure
$p_{i,max}$	Maximum injection pressure at the surface
p_r	Refracturing pressure
γ	Rock bulk density
δ_0	Initial reservoir pressure gradient
δ_c	Closing pressure gradient
δ_f	Fracturing pressure gradient
ε_h	Minimum horizontal principal stress gradient
ε_H	Maximum horizontal principal stress gradient
λ	Lateral stress coefficient
t	Time
T	Tensile strength of the rock around borehole
t_i	Injection time
t_{lp}	Last pumping time
t_s	Well shut-in time
Δt	Time interval between the two adjacent cycles
Temp	Temperature
V_i	Total injection volume
$v_{i,ave}$	Average injection rate at the surface
V_r	Backflow volume
σ_h	Minimum horizontal principal stress
σ_H	Maximum horizontal principal stress
σ_v	Vertical stress
$\Delta\sigma$	Effective stress difference changed from initial to some stressed state

1 Introduction

Coal seams are naturally fractured reservoirs with coalbed methane (CBM) consisting of matrix blocks, where most gas is adsorbed onto coal inner surfaces. A network of cleats, usually saturated with water in an in situ state, provide the major flow paths for gas and water in the coal seams (Clarkson and McGovern 2005; Pan and Connell 2012; Chen et al. 2014; Zhao et al. 2014). The magnitude and orientation of in situ stress can substantially influence coal deformation and destruction (including both cleat and matrix), and with increase of that stress, its role becomes

more prominent (Ryan 2003; Bell 2006; Liu et al. 2014). Clearly, in situ stress measurement in the downhole is indispensable for coal and CBM development (Iannacchione et al. 2007; Karacan et al. 2008; Gentzis 2009, 2011a, b; Chatterjee and Pal 2010; Meng et al. 2010; Liu 2011; Talebi et al. 2014).

In situ stress is a type of internal stress in the earth crust, and its formation is closely related to various dynamic actions during historical geologic periods, including gravitational and tectonic stresses (Cai et al. 2010; Kang et al. 2009, 2010). The gravitational stress field caused by rock mass gravity is relatively simple and can be estimated by the specific weight of overburden and buried depth. On the contrary, the tectonic stress field is much more complicated, and is greatly influenced by tectonic movements (especially in the horizontal) and rock geological structures. In addition, the tectonic stress field is extremely irregular in spatial distribution and almost impossible to describe by precise analytical solutions, because it is continually changing with geologic age (Kang et al. 2010). However, at the human scale these stresses (tectonic and gravitational) can be assumed constant. Only local changes in the in situ stress occur caused by the reservoir exploitation (Segall and Fitzgerald 1998; Jeanne et al. 2015).

During CBM development, accurate measurement of in situ stress is particularly important for coal reservoir permeability evaluation and CBM recoverability assessment (Haimson 2005; Paul and Chatterjee 2011; Li et al. 2014). Coal reservoir permeability is determined by the fracture system resulting from the ancient and current tectonic stress fields, which immediately affect fracture aperture, morphology and propagation (direction and dip) (Meng et al. 2011). Moreover, coal reservoir pressure or effective stress, coal matrix swell associated with gas adsorption (e.g., CBM or other gases injected in the coal reservoir), and shrinkage effects during CBM desorption and production also affect fracture aperture (White et al. 2005; Bustin et al. 2008; Kumar et al. 2010, 2012; Wang et al. 2011; Pan and Connell 2012; Singh et al. 2015). A series of permeability dynamic prediction models have been established by considering the aforementioned coal effective stress and matrix shrinkage effects (Palmer and Mansoori 1998; Shi and Durucan 2004; Connell et al. 2010; Pan and Connell 2012; Zhao et al. 2013). Nevertheless, these models are based on stress or strain that can be simulated in the laboratory and cannot be used to analyze the effect of in situ stress on CBM reservoir permeability, because of the contrasting time scales between CBM development and in situ stress variability. Recently, after revelations of successful CBM development in the United States (Johnson and Flores 1998; Nelson 2003; Tonnsen and Miskimin 2010), the government of China has

explored and developed CBM with great resource potential in the Ordos Basin. However, the ubiquitous characteristics of underpressured, CBM-undersaturated, low-porosity and low permeability in Chinese CBM reservoirs may cause coal reservoir permeability to be sensitive to stress change (Su et al. 2005; Yao et al. 2008; Keim et al. 2011; Xu et al. 2014). Moreover, both the complex stress conditions and poor reservoir properties could bring little economic benefit and inefficient development (Zhao et al. 2014). Chinese CBM development is mainly aimed at shallow coal seams, usually with depths 700–1000 m (Zhao et al. 2015a; Xu et al. 2015a, b; Lv et al. 2012; Li et al. 2014, 2015; Chen et al. 2014; Liu et al. 2014). Therefore, it is of major and practical significance to analyze the relationship between coal reservoir permeability, in situ stress and burial depth, which is beneficial to determine reasonable operating practice, reduce reservoir damage, improve CBM well productivity as well as guide deep CBM (>1000 m depths) exploration and development.

In this work, the data of reservoir pressure, in situ stress and well test permeability from 55 CBM wells were collected in the eastern margin of the Ordos Basin. Through statistics and regression analysis, correlations between stress, permeability and burial depth were determined to reveal the in situ stress distribution and address the impact of that stress on coal reservoir permeability, which is expected to provide theoretical support and guidance to CBM exploration and development.

2 Geological Setting

The eastern margin of the Ordos Basin crosses the Inner Mongolia Autonomous Region, Shanxi and Shaanxi provinces, and is a long and narrow zone along the Yellow River. This zone covers about $2.5 \times 10^4 \text{ km}^2$. It is nearly 560 km long in the north–south direction and 50–200 km wide in the east–west direction (Fig. 1). The zone has become the second most successful CBM development base after the Qinshui Basin since the 1980s (Xu et al. 2012a, b; Yang et al. 2013; Zhao et al. 2015b; Feng et al. 2015), and contains an estimated $9.0 \times 10^{12} \text{ m}^3$ of total CBM reserves that are buried less than 1500 m deep (Jie 2010). By the end of 2013, nearly 2000 CBM wells had been completed and vertical well productivity exceeded 6000 m^3/day ; that of horizontal wells reached 16,000 m^3/day (Chen et al. 2015).

The eastern margin of the Ordos Basin is composed of three tectonic units, the Jinxi fold, eastern Yimeng uplift, and eastern Weibei uplift (Xue et al. 2011; Tang et al. 2012) (Fig. 1). The area is a large west-dipping monocline with dip angle 3° – 10° , where the structures are relatively simple and stable. Only some slight northeast and north–

northeast trending folds and small-scale faults are developed, which are beneficial to CBM preservation and exploration (Yao et al. 2009; Jie 2010).

The main coal-bearing sequences in the area are in the Carboniferous Taiyuan and Permian Shanxi Formations. The coal-bearing strata are largely preserved, providing a good basis for CBM generation and accumulation (Chen et al. 2015). Figure 2 shows a geologic cross section of the two formations from south to north. There are more than 20 coal seams of various thicknesses, but their distribution is stable. The Taiyuan Formation is predominantly deposited in a tidal flat and delta system. The number of principal mineable coal seams ranges from 2 to 4 and the total number is between 4 and 8, with net coal thickness 3–40 m. The Shanxi Formation is mainly deposited in a shallow water delta, lagoon-gulf system consisting of three to nine coal seams. There are one to three major mineable coal seams that have general coal thickness approximately 4–15 m in total. Overall, coal thickness in the northern portion is the greatest (20–35 m), followed by 10–20 m in the central portion and <5 m in the south (Jie 2010). Average vitrinite reflectance of coal is from 0.44 to 2.35 % and the roof and floor of the major coal seams consist primarily of mudstone, sandy mudstone and sandstone (Jiang et al. 2012). These generally have low permeability and favorable CBM sealing effects, although the limestone roofs are usually aquifers that can dissolve gases and transport them out of the CBM reservoir in the Liulin block (Xu et al. 2015a).

3 Methodology

After a CBM well is completed and before it is put into production, the coal seam is usually tested to obtain parameters such as reservoir pressure, fracturing pressure, closing pressure, permeability and others, which can provide a reliable basis for regional CBM assessment. Generally, injection/falloff well testing accompanied by in situ stress measurement is done to obtain the above parameters (Li et al. 2014).

Injection/falloff is a type of transient well test that is usually conducted before in situ stress measurement basing on Chinese national standard GB/T 24504-2009 (AQSIO and SAC 2009). Throughout the test, because the formation pressure is always higher than the CBM critical desorption pressure, the fluid just maintains single-phase water flow in the cleats. Permeability of the coal matrix is much lower than that of the cleats, which demonstrates that the measured permeability is mainly from the cleats rather than the coal matrix. Here, two methods are available to examine well test data, including characteristic straight line analysis and chart board matching analysis. Usually, the selected analysis model is determined by the log–log curve

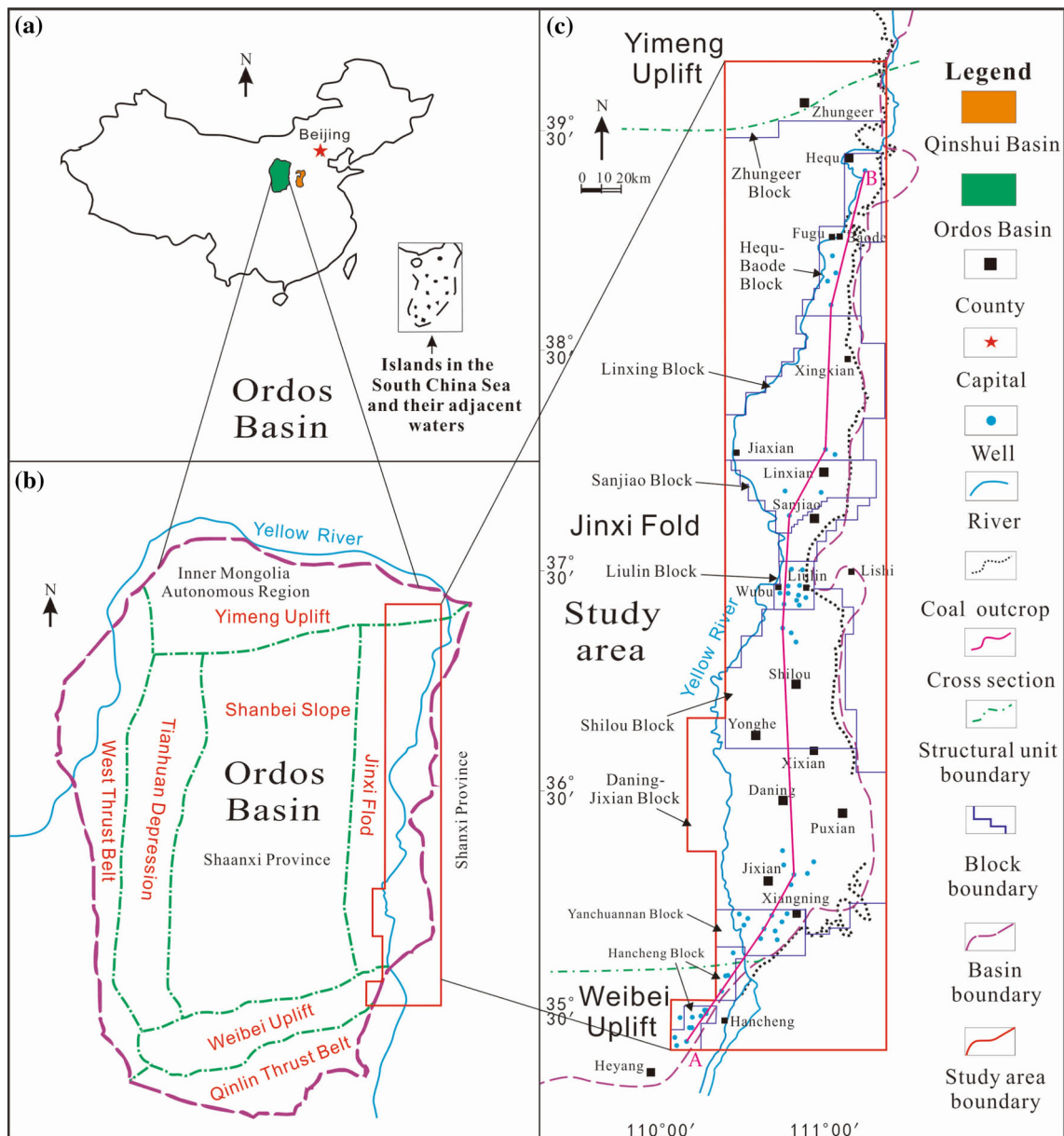


Fig. 1 Location of the eastern margin of the Ordos Basin, China. **a** Locations of the Qinshui and Ordos Basins in the China Map; **b** general location of the eastern margin of the Ordos Basin in the

tectonic division map; **c** specific locations of the CBM blocks and wells in the eastern margin of the Ordos Basin; *AB* is the cross section from south to north

characteristic of test data. If the log–log pressure derivative curve appears as a horizontal straight line segment in the middle period, the semi-log method can be used to calculate reservoir permeability. Other cases could be investigated by typical curve fitting (Hopkins et al. 1998). In the present work, to ensure that the parameters are accurate and reliable, pressure history matching curves were compared and verified with measured curves. Figure 3 shows the workflow for the permeability calculation with the injection/falloff data. Figure 4 portrays the injection/falloff curves of an actual CBM well.

It should be noted, however, that the maximum injection pressure at the surface before an injection/falloff well test is usually unknown for a new area or areas with less data. Consequently, a minifrac is typically required to determine that pressure (Meng et al. 2010, 2011; Li et al. 2014). Figure 5 shows minifrac curves of an actual CBM well. During an injection/falloff well test, to reduce damage from stress on reservoir permeability, injection pressure at the surface is initiated at a relatively low value, and the maximum injection pressure at the injection rate is kept lower than fracturing pressure during the designed

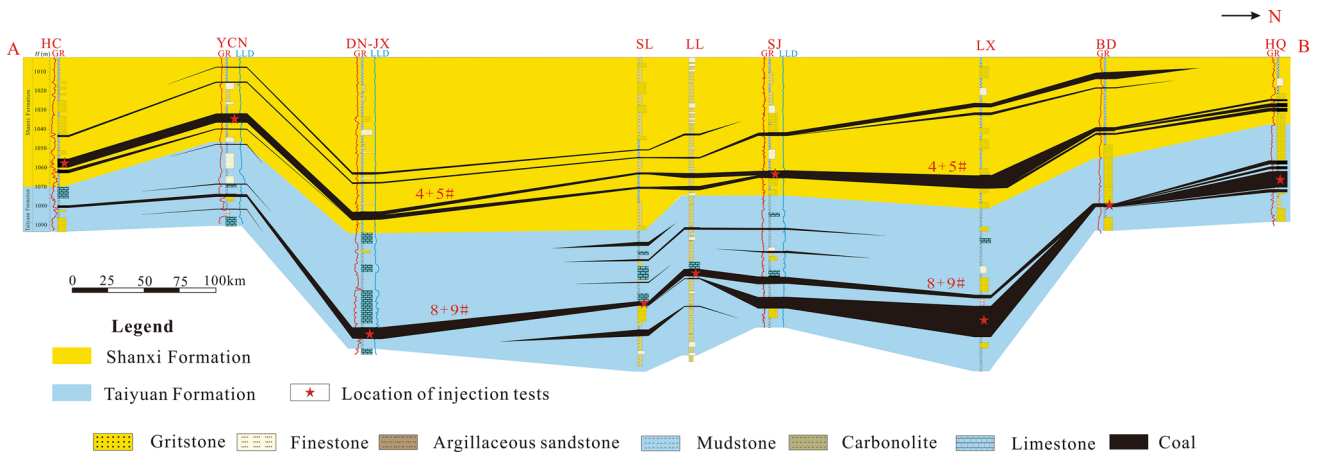


Fig. 2 A geologic cross section (AB) from south to north showing the Permian Shanxi and Carboniferous Taiyuan Formations (the section line could be found in Fig. 1c; GR gamma ray, LLD deep lateral resistivity, HC Hancheng block, YCN Yanchuannan block, DN-JX

Daning–Jixian block, SL Shilou block, LL Liulin block, SJ Sanjiao block, LX Linxing block, BD Baode block, HQ Hequ block; the 4 + 5# and 8 + 9# are the coal seam numbers of Shanxi and Taiyuan Formations, respectively)

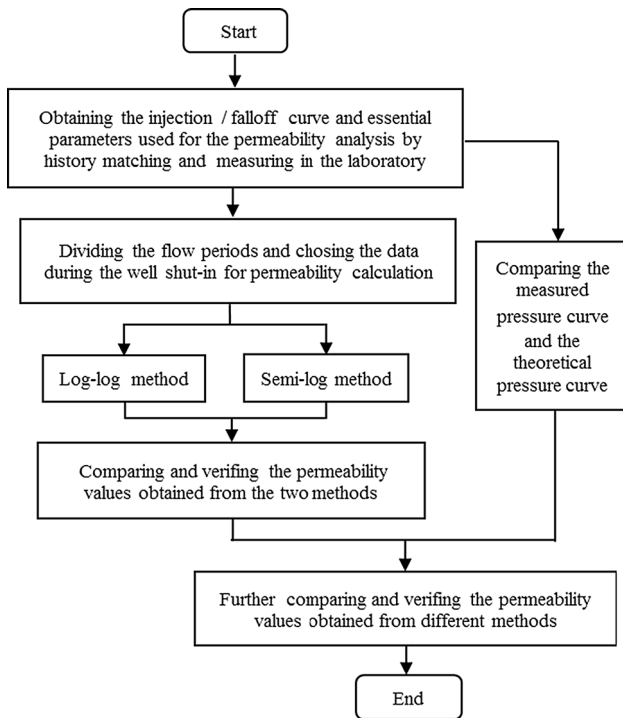


Fig. 3 Workflow for the permeability calculation with the injection/falloff well test data

injection period. The injection period should be longer than the end time of the wellbore storage effect, and the well shut-in time should not be shorter than twice the injection period. In the present study, flow-static injection was continued for 12 h and the well was then shut in for at least 24 h to obtain the curves between temperature, pressure and time. Those curves were used to calculate reservoir permeability and initial reservoir pressure (Fig. 4).

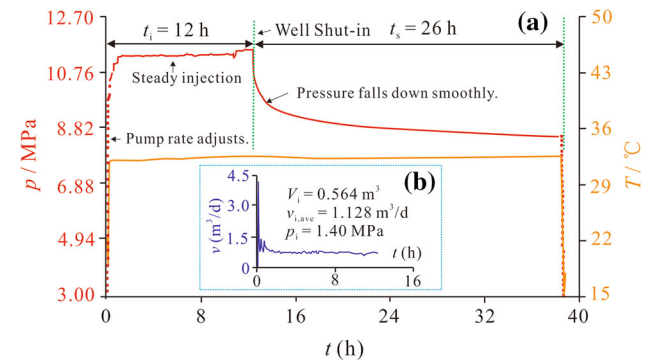


Fig. 4 Injection/falloff curves of an actual CBM well. **a** Relationship between the pressure/temperature and time; **b** relationship between the injection rate at the surface and time; V_i represents the total injection volume; $v_{i,ave}$ represents the average injection rate at the surface; p represents the pressure; p_i represents the injection pressure; t represents the time; t_i represents the injection time; t_s represents the well shut-in time

In situ stress is often measured by the multi-cycle hydraulic fracturing method (Hubbert and Willis 1957; Kang et al. 2010; Liu et al. 2014; Li et al. 2014, 2015), according to Chinese earthquake industry standard DB/T 14-2000 (CEA 2000), which is also appropriate for the in situ stress measurement of coal (Kang et al. 2010; Liu et al. 2014), following the injection/falloff well test (Li et al. 2014, 2015). During the in situ stress measurement, the objective of pumping a thin fluid (water) at a certain rate into the target coal seam is to create a small fracture. Initially, pressure in the fracture is less than the fracture closing pressure and the fracture is closed. When the pressure in the fracture is greater than the fracture closing pressure, the fracture opens. Once this occurs, the pumps are shut down and the pressure falloff with time is

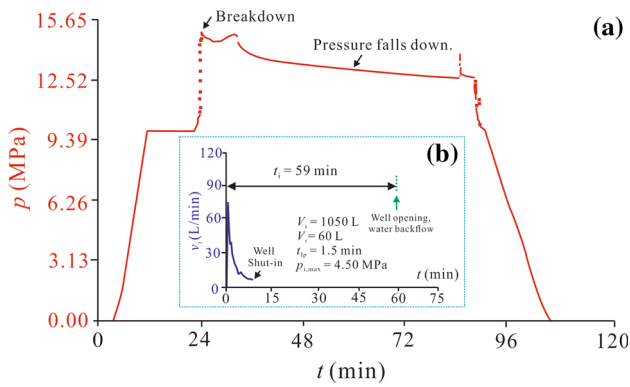


Fig. 5 Minifrac curves of an actual CBM well. **a** Relationship between the pressure and time; **b** relationship between the injection rate at the surface and time; $p_{i,max}$ represents the maximum injection pressure at the surface; V_r represents the backflow volume; t_{ip} represents the last pumping time

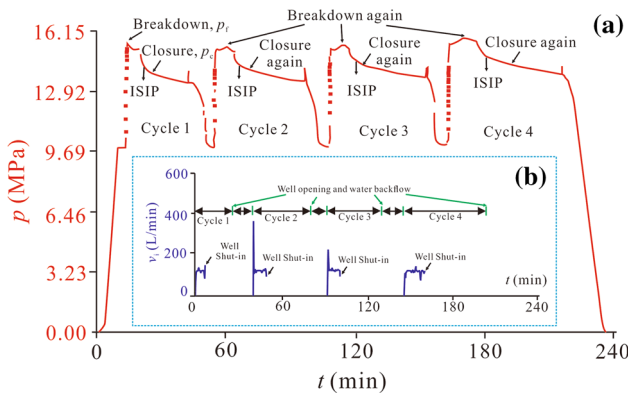


Fig. 6 In situ stress measurement and injection rate curves of an actual CBM well. **a** Relationship between the pressure and time; **b** relationship between the injection rate and time at the surface; ISIP represents the instantaneous shut-in pressure; p_f represents the fracturing pressure; p_c represents the closing pressure

recorded. When the fracture closes, the fracture closing pressure is equal to the minimum horizontal stress. This is why stresses can be deduced from the fluid injection test. Therefore, through the injection curve, reservoir fracturing pressure can be obtained. With the falloff curve, reservoir fracture closing pressure can be calculated (Zuber et al. 1990). During in situ stress tests, two to three cycles with clear fracturing and closing effects were chosen to calculate in situ stress parameters with the time square root method (Li et al. 2014), and were further verified by the log–log method. Figure 6 reveals the in situ stress measurement curves of an actual CBM well.

For the in situ stress measurement of a vertical well, when the formation pressure increases to the fracturing pressure by injecting water after the perforation is packed, the maximum horizontal principal stress can be expressed as (Bredehoeft et al. 1976):

$$\sigma_H = 3p_c - p_f - p_0 + T, \quad (1)$$

where, σ_H is the maximum horizontal principal stress, MPa; p_c is the closing pressure, MPa; p_f is the fracturing pressure, MPa; p_0 is the rock pore pressure (initial reservoir pressure); T is tensile strength of the rock around the borehole, MPa.

If the fluid is injected continuously to pressurize the reservoir, the fracture will extend to the deep site. Otherwise, if fluid injection is halted and the fracturing loop is kept closed, the fracture will immediately stop expanding and tend to close. Here, the balance pressure that can just keep the fracture open is called closing pressure and is equivalent to the minimum horizontal principal stress perpendicular to the fracture surface (Haimson and Fairhurst 1970; Haimson and Cornet 2003), i.e.,

$$\sigma_h = p_c, \quad (2)$$

where σ_h is the minimum horizontal principal stress, MPa.

Similarly, if the injection process is repeated, the fracture will reopen and the refracturing pressure will be attained. Because the rock has been fractured, the rock tensile strength equals 0 and the fracturing pressure can be written as

$$p_f(T = 0) = p_r = 3\sigma_h - \sigma_H - p_0, \quad (3)$$

where p_r is the refracturing pressure, MPa.

Substituting Eqs. (2) and (3) into Eq. (1), rock tensile strength is expressed as

$$T = p_f - p_r \quad (4)$$

The vertical principal stress can be computed according to the weight of overlying rock from 116 in situ stress test results worldwide (Hoek and Brown 1980), yielding the prediction equation of that stress used herein:

$$\sigma_v = 3\gamma H \approx 0.027H \quad (5)$$

where, σ_v is the vertical principal stress, MPa; γ is rock bulk density, kN/m^3 ($1 \text{ kN/m}^3 = 0.001 \text{ MPa/m}$); H is burial depth, m.

During the in situ stress tests, tubing strings are used to lower the bottom-hole pressure gauge, packer and shut-in tools into the well. The packer is installed on an immediate roof that can be identified by logging data. Through the pipelines, underground equipment is connected with the injection system at the surface. In a short time, the injection fluid (formation water or filtered clean water) is pumped into the wellbore at a high rate, which makes the flowing bottom-hole pressure higher than the fracturing pressure of the target strata. Once the target strata fracture, the tested well is shut in and then the falloff curve may be acquired from the falloff data (Fig. 7).

To accurately estimate the in situ stress and eliminate uncertainties in the measurements, four cycles were

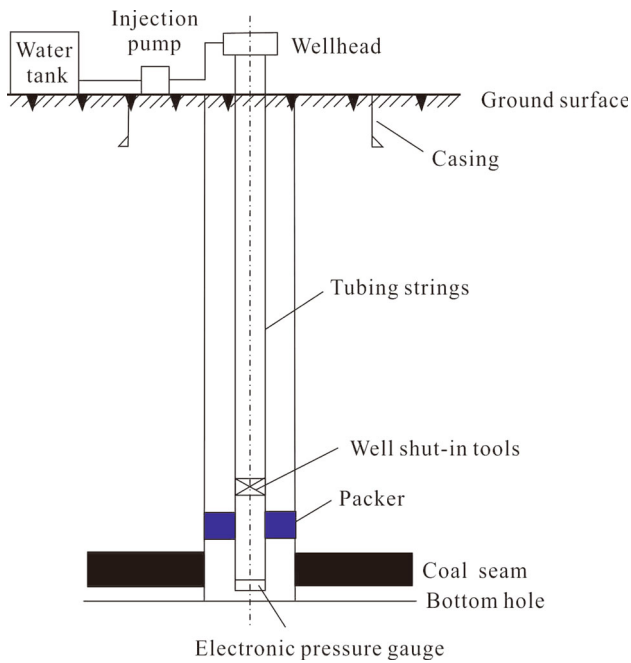


Fig. 7 Schematic diagram of the in situ stress measurement

performed in the hydraulic fracturing and all in situ stress data were calculated on the basis of the hydraulic fracturing test. The general measurement steps are as follows: (1) starting the injection pump at the surface and injecting water into the well at a certain rate with the ladder displacement method; (2) observing change of wellhead pressure until fracture occurrence after pumping 2–6 min continuously, shutting in the well for 20 min and measuring the reservoir pressure drop; (3) opening the well again and recording backflow volume; (4) keeping the injection rate as in the first cycle and running another 2–4 cycles per the designed injection and shut-in time; (5) comparing the measured and pressure gauge data and if the former is qualified, ending the in situ stress test (Fig. 6). Table 1 shows in situ stress measurement data from an actual CBM well in the eastern margin of the Ordos Basin.

4 Results and Discussions

4.1 Results of In Situ Stress and Injection/Falloff Well Tests

The in situ stress data measured by four-cycle hydraulic fracturing of 55 CBM wells in the eastern margin of the Ordos Basin indicates that at coal seam burial depths (H) 455.60–1323.10 m (average 832.46 m), initial reservoir pressure (p_0) is 2.58–12.22 MPa (average 6.73 MPa) and the pressure gradient (δ_0) 0.40–1.42 MPa/100 m (average 0.82 MPa/100 m), which represents an predominant

Table 1 In situ stress measurement data of an actual CBM well in the eastern margin of the Ordos Basin

Parameters	Cycle number			
	1	2	3	4
V_i (L)	865	1215	1195	1775
V_r (L)	190	285	350	525
$p_{i,max}$ (MPa)	5.50	5.30	5.30	5.80
t_i (min)	7.00	9.25	8.95	14.50
t_{ip} (min)	4.50	2.25	5.20	4.00
t_s (min)	20.00	30.00	30.00	40.00
Δt (min)	0.00	14.00	14.00	15.00

V_i represents the total injection volume, L; V_r represents the backflow volume, L; $p_{i,max}$ represents the maximum injection pressure, MPa; t_i represents the injection time, min; t_s represents the well shut-in time, min; t_{ip} represents the last pumping time, min; Δt represents the time interval between the two adjacent cycles, min

underpressured reservoir. The closing pressure (p_c) is 6.98–26.88 MPa (average 15.04 MPa) and the pressure gradient (δ_c) 1.22–2.94 MPa/100 m (average 1.83 MPa/100 m). The coal seam fracturing pressure (p_f) is 8.17–31.08 MPa (average 16.39 MPa) and the pressure gradient (δ_f) 1.32–3.35 MPa/100 m (average 1.99 MPa/100 m) (Fig. 8; Table 2). Overall, the burial depth in this area is greater than that of the Qinshui Basin which is accompanied by lower initial reservoir pressure, closing pressure and fracturing pressure (Fig. 9; Table 2, Meng et al. 2010). Coal reservoir temperature is 16.08–45.37 °C with average 32.01 °C (Fig. 8; Table 3).

With Eqs. (1), (2) and (5), magnitudes of the maximum and minimum horizontal principal stresses and the vertical principal stress were computed. This shows that the maximum horizontal principal stress (σ_H) is 10.13–37.84 MPa with average 22.50 MPa [its stress gradient (ϵ_H) is 1.43–4.13 MPa/100 m with average 2.75 MPa/100 m]. The minimum horizontal principal stress (σ_h) is 6.98–26.88 MPa with average 15.04 MPa, for which the stress gradient (ϵ_h) is 1.22–2.94 MPa/100 m with average 1.83 MPa/100 m. The vertical principal stress (σ_v) is 12.30–35.72 MPa with average 22.48 MPa (Fig. 8; Table 3). Compared with the Black Warrior Basin in the United States (where minimum horizontal principal stress is generally 1–6 MPa, McKee et al. 1988) and the Sydney and Bowen Basins in Australia (minimum horizontal principal stress generally 1–10 MPa, with a few values of 14 MPa, Enever and Henning 1997), in situ stress is greater in the coal seams in the eastern margin of the Ordos Basin. Overall, that stress is moderate to strong, because 85 % of the stresses are 10–30 MPa according to the assessment standard (Kang et al. 2009).

Similar to the Qinshui Basin, the initial reservoir pressure, fracturing pressure, and closing pressure all have a

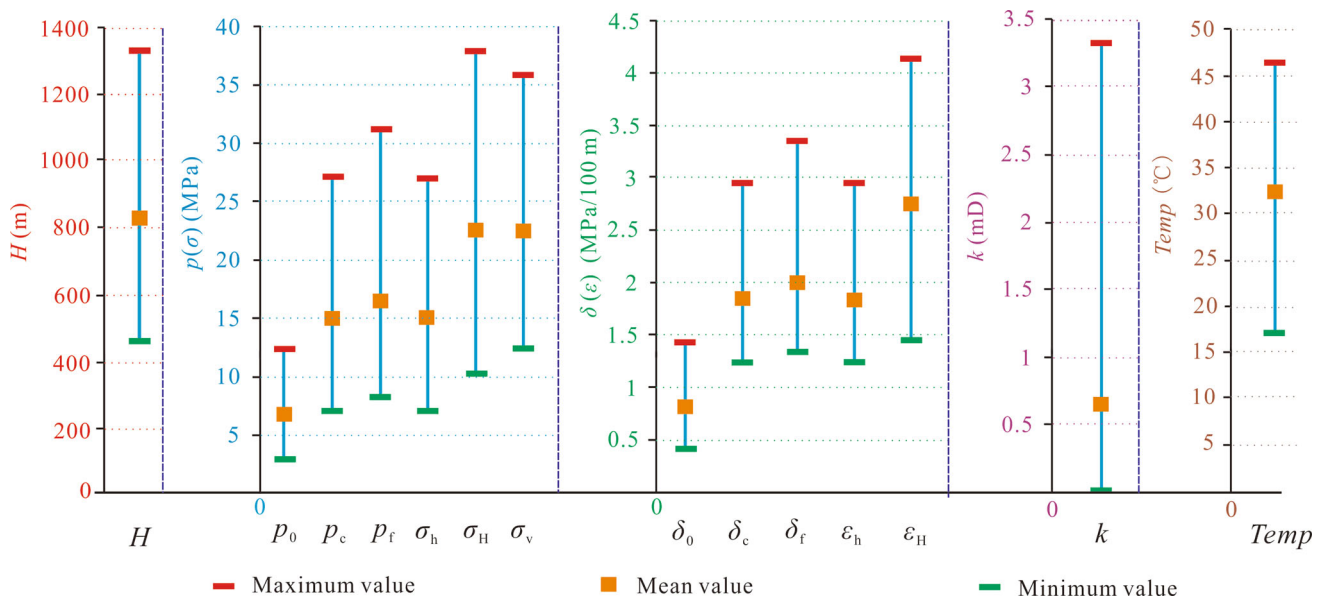


Fig. 8 Stock chart of injection/falloff well test and in situ stress measurement parameters in the Ordos Basin (H represents the burial depth; p_0 represents the initial reservoir pressure; σ_H represents the maximum horizontal principal stress; σ_h represents the minimum horizontal principal stress; σ_v represents the vertical stress; δ_0 represents the initial reservoir pressure gradient; δ_c represents the

closing pressure gradient; δ_f represents the fracturing pressure gradient; ε_h represents the minimum horizontal principal stress gradient; ε_H represents the maximum horizontal principal stress gradient; Temp represents the reservoir temperature; k represents the permeability)

linearly increasing trend with increase of coal burial depth (Fig. 10a–c, Meng et al. 2010). The relevant relationships are as follows.

1. Initial reservoir pressure:

$$p_0 = 0.0064H + 1.3849 \quad (6)$$

2. Fracturing pressure:

$$p_f = 0.0168H + 2.368 \quad (7)$$

3. Closing pressure:

$$p_c = 0.0147H + 2.7772 \quad (8)$$

Moreover, the fracturing pressure has a clear positive correlation with closing pressure (Fig. 10d), expressed as

$$p_c = 0.8324p_f + 1.396 \quad (9)$$

The results of the injection/falloff well tests indicate that coal reservoir permeability is 0.01–3.33 mD with average 0.65 mD, and 75 % of values are <1 mD. This reveals that the coal seam is a typical low permeability reservoir (Fig. 8; Table 3).

4.2 Principal Stress Variation with Depth

Figure 11 shows that the maximum and minimum horizontal principal stresses and the vertical principal stress are all positively correlated with buried depth. Because the minimum horizontal principal stress has a strong and even decisive impact on the fracturing pressure and its gradient

and limits the expansion of hydraulic fractures, this stress becomes one of the key parameters in CBM well drilling design and coal seam reinforcement (Tang et al. 2011; Hallam and Last 1991; Hubbert and Willis 1957). In a common sedimentary basin, this stress is typically ~70 % of the vertical stress (Meng et al. 2013). However, 70 % of the coal reservoir vertical stress cannot accurately describe the magnitude and variation of the minimum horizontal principal stress in the eastern margin of the Ordos Basin. For example, at depths >1000 m, 70 % of the vertical stress is larger than the minimum horizontal principal stress. Overall, the minimum horizontal principal stress in the coal reservoir is slightly weaker than that of sedimentary rock strata in a common sedimentary basin. This is mainly attributed to coal as the organic matter and its weaker mechanical strength.

Based on the actual data, a general trend of the in situ stress change can be observed and in the vertical direction, stress field types in the study area are as follows. At depths <700 m, the coal reservoir in situ stress state is such that $\sigma_H > \sigma_v > \sigma_h$, the minimum horizontal principal stress is <19 MPa, and the current in situ stress field type is a strike slip regime. At depths 700–1000 m, the coal reservoir in situ stress state changes to $\sigma_H \approx \sigma_v > \sigma_h$, indicating a stress transition zone where the average minimum horizontal principal stress is ~15 MPa. In the deep coal seam with burial depths >1000 m, vertical stress increases conspicuously and is greater than the maximum principal

Table 2 CBM reservoir parameters associated with in situ stress in the Qinshui and Ordos Basins

Basin	H (m)	p_0 (MPa)		P_F (MPa)		P_c (MPa)	
		p_0 (MPa)	δ_0 (MPa/100 m)	p_f (MPa)	δ_f (MPa/100 m)	p_c (MPa)	δ_c (MPa/100 m)
Ordos Basin	455.60–1323.10 (823.46)	2.85–12.22 (6.73)	0.40–1.42 (0.82)	8.17–31.08 (16.39)	1.32–3.35 (1.99)	6.98–26.88 (15.04)	1.22–2.94 (1.83)
Qinshui Basin	334.90–1122.30 (590.85) ^a	1.34–10.60 (4.41)	0.28–1.08 (0.71)	6.44–27.74 (12.21)	1.49–2.96 (2.01)	3.30–26.40 (10.51)	0.99–2.85 (1.70)
	429.00–1077.65 (670.36) ^b	2.67–12.63 (5.42)	0.46–1.18 (0.78)	10.30–23.60 (14.62)	1.62–2.71 (2.17)	8.00–20.76 (12.51)	1.37–2.26 (1.85)

p_f represents the fracturing pressure MPa; p_c represents the closing pressure, MPa; p_0 represents the initial reservoir pressure, MPa; δ_0 represents the initial reservoir pressure gradient, MPa/100 m; δ_c represents the closing pressure gradient, MPa/100 m; δ_f represents the fracturing pressure gradient, MPa/100 m

^a Shanxi Formation

^b Taiyuan Formation in the Qinshui Basin; the data format is minimum–maximum and the data in the brackets represents the average value

stress, i.e., $\sigma_v > \sigma_H > \sigma_h$, with the minimum principal stress increasing from 14.80 to 26.88 MPa and averaging 19.88 MPa. These strata show a normal stress regime type, which is advantageous for normal fault activity and indicates an extension zone (Anderson 1951, Fig. 11).

4.3 Principal Stress Ratio Variation with Depth

Generally, when researching the stress field change behavior, the lateral stress coefficient is used to represent the in situ stress state at some point (Brown and Hoek 1978; Hoek and Brown 1980; Han et al. 2012). The lateral stress coefficient is defined as the ratio of average horizontal principal stress to vertical stress, expressed as

$$\lambda = \frac{\sigma_H + \sigma_h}{2\sigma_v}, \tag{10}$$

where, λ is the lateral stress coefficient.

Measurements of lateral stress coefficient in the eastern margin of the Ordos Basin indicate that this parameter ranges from 0.51 to 1.21 with average 0.84. These values are between the Hoek–Brown inner and outer in situ stress envelopes representing the relationship between the ratio and burial depth worldwide (Brown and Hoek 1978) and those in China (Zhao et al. 2007) (Fig. 12). At depths <700 m, the lateral stress coefficient variation is 0.61–1.21 with average 0.94. The lateral stress coefficient is 0.51–1.12 with average 0.82 for 700–1000 m depths. For depths >1000 m, that coefficient is 0.62–0.98 with average 0.76. The lower limit of the in situ stress transformation depth corresponding to the depth at which the lateral stress coefficient equals 1 appears around 900 m, just within the range 700–1000 m. In other words, at depths <900 m, the horizontal principal stress is dominant and the lateral stress coefficient is large and disperse. The vertical principal stress is primary at depths >900 m where the lateral stress coefficient converges. This result is consistent with the analysis of Brown and Hoek (1978) and Zhao et al. (2007), who discussed lateral stress coefficient variation with depth worldwide and in China, respectively.

Referencing the expression of the Hoek–Brown inner and outer envelopes, the lateral stress coefficient is rewritten in the following form:

$$\lambda = \frac{a}{H} + b, \tag{11}$$

where, a and b are undetermined coefficients, respectively.

Equation (11) shows a linear relationship between the lateral stress coefficient and reciprocal of the buried depth. Thus, by regression of the measured lateral stress coefficients after linearizing the data, the trend line and inner and outer in situ stress envelopes of the eastern margin of the Ordos Basin were obtained. From Fig. 12, the outer

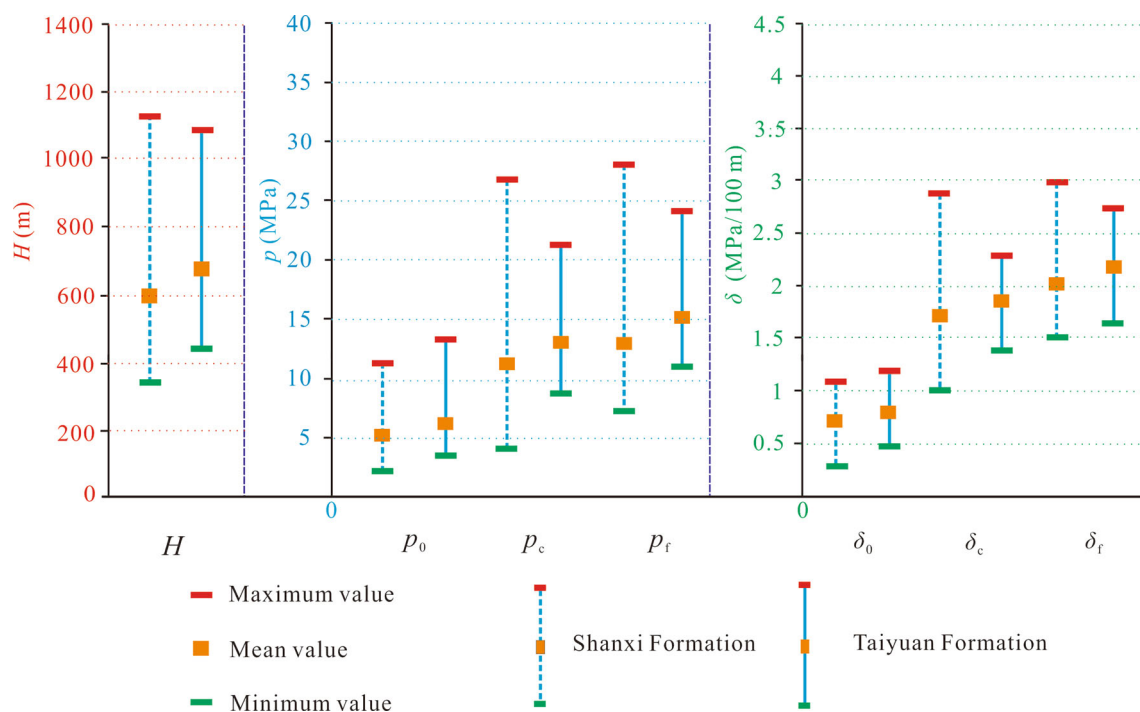


Fig. 9 Stock chart of injection/falloff well test and in situ stress measurement parameters in the Qinshui Basin (based on Meng et al. 2010)

envelope in the area is basically coincident with the Hoek–Brown outer envelope. The inner envelope is within the Hoek–Brown inner envelope and essentially coincident with the Chinese in situ stress inner envelope, indicating that the in situ stress measurements from the hydraulic fracturing method are credible.

Furthermore, by similar linear regression of the stress ratios and burial depth, trend lines of the ratios and their general ranges at various depths were acquired (Fig. 13). It is seen that the ratios of horizontal principal stresses in the study area are 1.08–1.70 with average 1.48. The ratios of maximum principal stress to vertical principal stress are 0.53–1.53 with average 1.01, and ratios of minimum principal stress to vertical principal stress are 0.45–0.90 with average 0.67. Overall, the three in situ stress ratios slowly decreased with buried depth. At <700 m depths, variation of the three ratios is great and their decrease with burial depth is rapid. For 700–1000 m depths, that decrease slows substantially, and is near zero at depths >1000 m. This general change behavior is consistent with the analysis of Liu et al. (2014), who addressed lateral stress coefficient variation with depth in the Huainan coalfield.

4.4 Permeability Variation Under the Principal Stress

Permeability is one of the key determinants of CBM productivity (Wang et al. 2011, 2013). Coal reservoir

permeability is extremely sensitive to in situ stress and with increase of that stress, the permeability decreases exponentially (Somerton et al. 1975). This has been verified by field measurements, e.g., in coal of the Australian Sydney and Bowen Basins (Enever and Henning 1997; Enever et al. 1998), the American San Juan, Piceance and Black Warrior Basins (McKee et al. 1988; Sparks et al. 1995), and the Chinese Qinshui Basin (Meng et al. 2011). Generally, in situ stress has clear effects on coal reservoir permeability. When other factors (e.g., coal pore-fracture structures, petrographic constituents, and engineering operations) are equal, the greater stress could bring the lower the permeability and the poorer the CBM well productivity. In such a case, permeability may be roughly determined based on in situ stress magnitude (Li et al. 2014).

In our study, a negative exponent was used to analyze the relationship between coal reservoir well test permeability and in situ stress (Seidle et al. 1992; Zhao et al. 2015b), as

$$k = k_0 e^{-\alpha \Delta \sigma}, \quad (12)$$

where, k is permeability of a given stress condition, mD; k_0 is permeability of the initial stress condition, mD; $\Delta \sigma$ is the effective stress difference between an initial and a given stressed state, MPa; α is a coefficient dependent on the principal stress type.

Table 3 Injection/falloff and in situ stress test parameters in the eastern margin of the Ordos Basin

Basin	H (m)	σ_h		σ_H		σ_v (MPa)	K (mD)	Temp ($^{\circ}C$)
		σ_h (MPa)	ϵ_h (MPa/100 m)	σ_H (MPa)	ϵ_H (MPa/100 m)			
Ordos Basin	455.60–1323.10 (823.46)	6.98–26.88 (15.04)	1.22–2.94 (1.83)	10.13–37.84 (22.50)	1.43–4.13 (2.75)	12.30–35.72 (22.48)	0.01–3.33 (0.65)	16.08–45.37 (31.47)

σ_H represents the maximum horizontal principal stress, MPa; ϵ_h represents the minimum horizontal principal stress, MPa; σ_v represents the vertical stress, MPa; ϵ_H represents the minimum horizontal principal stress gradient, MPa/100 m; ϵ_h represents the maximum horizontal principal stress gradient, MPa/100 m; Temp represents the reservoir temperature, $^{\circ}C$; k represents the permeability, mD; the data format is minimum–maximum and the data in the brackets represents the average value

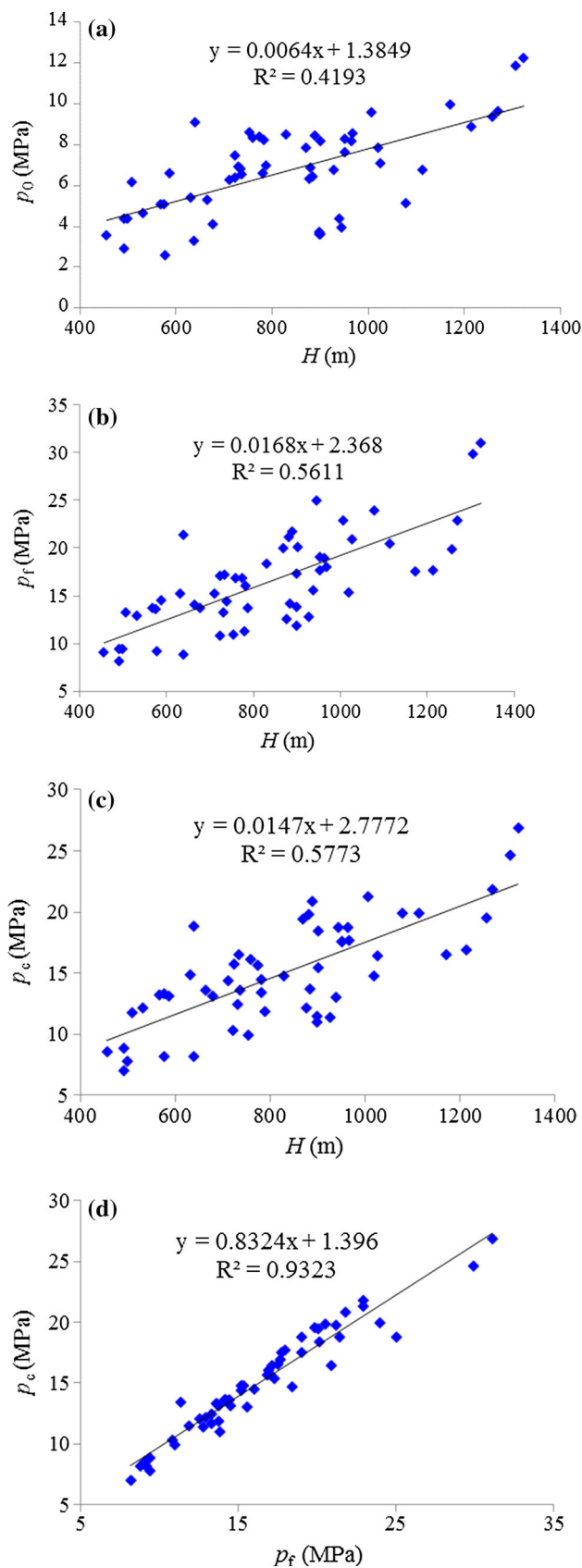


Fig. 10 Scatter diagrams of coal reservoir pressure, fracturing pressure, closing pressure and burial depth

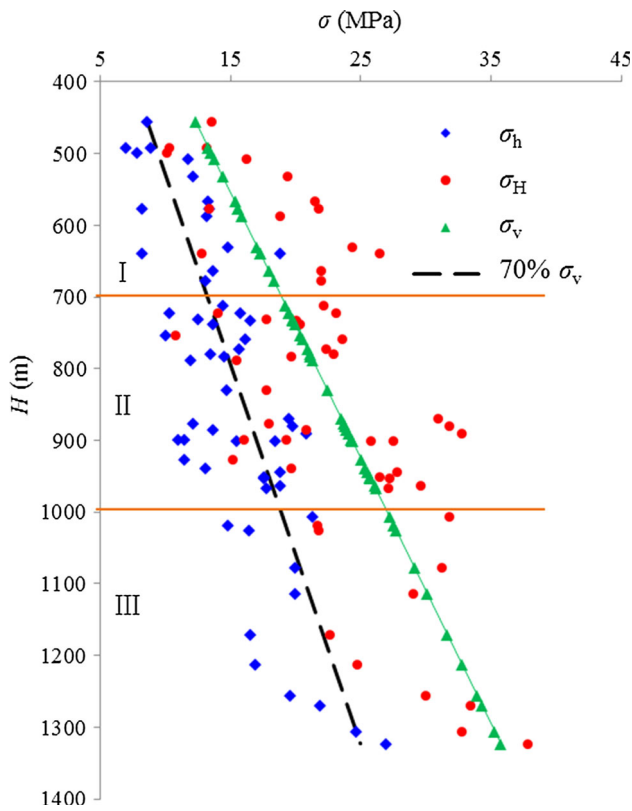


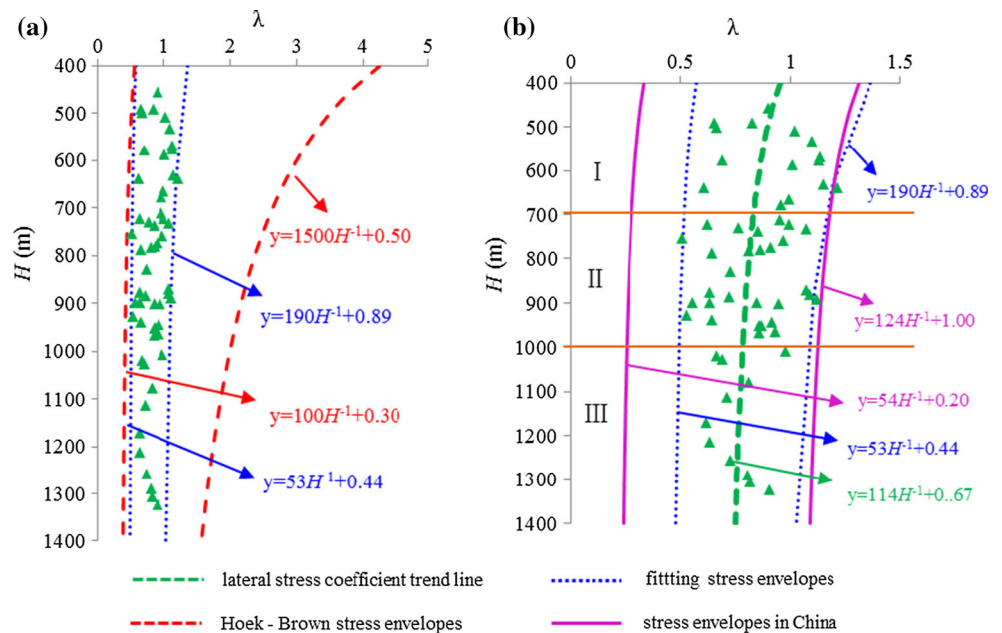
Fig. 11 Scatter diagrams of maximum horizontal principle stress, minimum horizontal principle stress, vertical principle stress and burial depth (*I* represents $\sigma_H > \sigma_v > \sigma_h$ where the horizontal principal stress is dominant revealing a strike slip regime; *II* represents $\sigma_H \approx \sigma_v > \sigma_h$ showing a stress transition zone; *III* represents $\sigma_v > \sigma_H > \sigma_h$ which indicates that the vertical principal stress is dominant demonstrating a normal stress regime)

Figure 14 shows that a decreasing behavior can describe the relationship between the maximum horizontal principal stress and coal reservoir permeability. The same applies to the minimum horizontal principal stress. This result is in accord with correlations between the measured permeability of coal seam and in situ horizontal stresses in the Hancheng and Liulin blocks in the eastern margin of the Ordos Basin, found by Tang (2001) and Li et al. (2014), respectively. After ~ 20 MPa in Figs. 14a and 15 MPa in Fig. 14b, high permeability data disappears. In contrast, the relationship between permeability and vertical principal stress is relatively complicated. With increasing stress, the permeability shows a tendency of decrease (<20 MPa), increase ($20\text{--}25$ MPa) and decrease (>25 MPa). When that stress is >30 MPa, the permeability is extremely low. This permeability change is in accord with Li et al. (2014, 2015).

In fact, the above permeability variation with vertical principal stress represents the relationship between permeability and burial depth, as that stress is calculated by Eq. (5). Figure 15 indicates that the permeability has three distinct vertical bands with increase of buried depth. At depths <700 m, the permeability decreases with buried depth and is 0.01–3.33 mD with average 0.89 mD. For 700–1000 m depths, permeability increases with depth and is 0.01–3.26 mD with average 0.73 mD. At depths >1000 m, permeability is very low, at 0.01–0.42 mD with average 0.11 mD.

Taking the stress variation into consideration, coal reservoir permeability inflection points at various depths are basically consistent with transition points of the stress field types and states at corresponding depths (Meng et al.

Fig. 12 Scatter diagrams of coefficient of lateral stress and burial depth. **a** Relationship between the lateral stress coefficient and the Hoek–Brown stress envelopes; **b** the relationship between the lateral stress coefficient and the stress envelopes in China



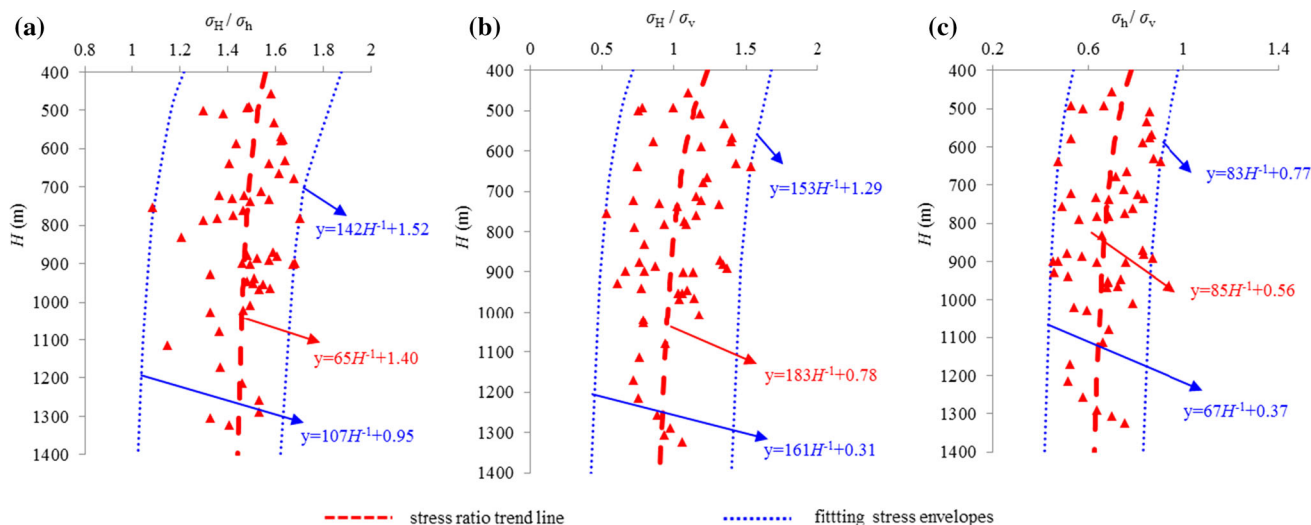


Fig. 13 Scatter diagrams of in situ stress ratios and burial depth. **a** Relationship between the ratio of the horizontal principal stresses and the burial depth; **b** relationship between the ratio of the maximum principal stress to the vertical principal stress and the burial depth; **c** relationship between the ratio of the minimum principal stress to the vertical principal stress and the burial depth

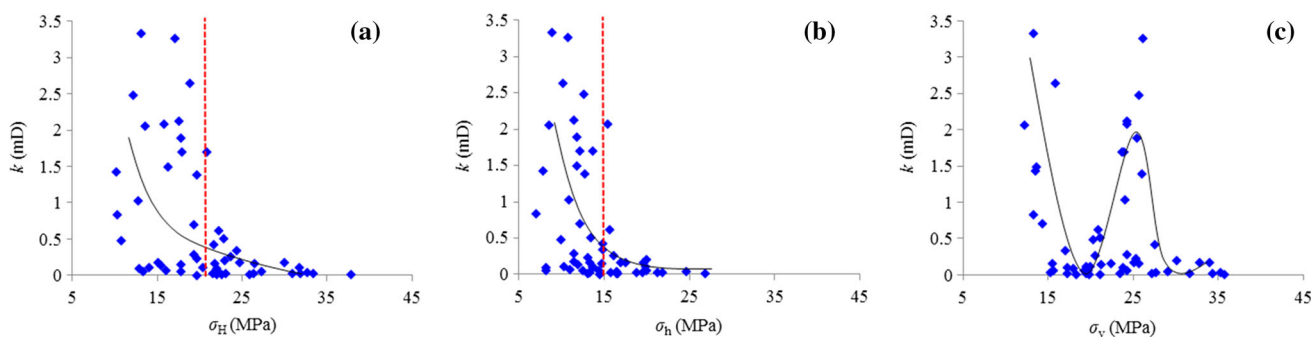


Fig. 14 Scatter diagrams of in situ stresses and well test permeability. **a** Relationship between the maximum horizontal principal stress and the permeability; **b** relationship between the minimum principal stress and the permeability; **c** relationship between the vertical principal stress and the permeability

2011). In this work, for coal seams at burial depths <700 m, the horizontal principal stress is dominant. There, coal fractures gradually close and permeability decreases gradually with burial depth, corresponding to increase of the in situ stresses. During in situ stress state transitions (700–1000 m), with further increase of those stresses, both elastic and some inelastic deformation may occur. This results in part of the pores and fractures opening, because of friction and slide of the fractures or even coal destruction. Therefore, in this in situ stress transition zone, the stress-dependent permeability somewhat increases. Nonetheless, permeability of the coal seams buried more than 1000 m deep decreases rapidly instead of continuously increasing, although it is an extensional stress regime where the rock is in a compressive state but the vertical compressive stress is higher than the horizontal compressive stress. The main reason

for this is that under the stronger vertical principal stress in a deep coal seam, the coal reservoir pore and fracture system tends to close again and cannot be effectively connected which results a rapid permeability reduction. Obviously, the essential influence of deep burial on permeability is its control by in situ stress control, i.e., the deformation and destruction of coal pore structures under in situ stress. This is consistent with Li et al. (2014, 2015), who discovered the same situation.

Finally, in the eastern margin of the Ordos Basin, optimizing the relationships among buried depth, in situ stress and permeability is very important for improvement of CBM productivity. Moreover, deep-level (>1000 m) CBM development faces the extreme challenge of “extremely low permeability and extremely high in situ stress,” which is the current problem in need of urgent solution for CBM development in China.

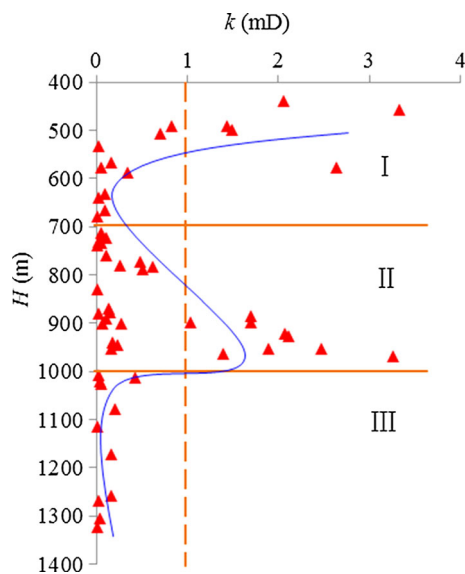


Fig. 15 Scatter diagrams of well test permeability and burial depth

5 Conclusions

Through the regression of measured injection/falloff and in situ stress well test data for 55 CBM wells in the eastern margin of the Ordos Basin, the distribution of in situ stress and its effect on permeability were analyzed systematically.

1. The maximum and minimum horizontal principal stress and vertical principal stress are all positively correlated with buried depth. Stress ratios and the lateral stress coefficient have a slow attenuation trend with buried depth.
2. Overall, there are three in situ stress states in the eastern margin of the Ordos Basin. At burial depths <700 m, the in situ stress state is $\sigma_H > \sigma_v > \sigma_h$, revealing a strike slip regime. From 700 to 1000 m depths, $\sigma_H \approx \sigma_v > \sigma_h$, showing a stress transition regime. At depths >1000 m, the in situ stress state changes to $\sigma_v > \sigma_H > \sigma_h$ demonstrating a normal stress regime.
3. Well test permeability decreases with horizontal principal stress but has a decrease–increase–decrease trend with increased vertical stress. This is basically consistent with the change of stress state at a certain burial depth, whose essence is the deformation and destruction of coal pore structures under the action of stresses.
4. With increase of buried depth, the vertical principal stress gradually dominates. A state of “extremely low permeability and extremely high in situ stress” means that it is very difficult to develop the deep-level CBM resource (>1000 m depths).

Acknowledgments This work was financially supported by the National Natural Science Foundation Project (Grant Nos. 41272175, 41530314), the Special Funds for Scientific Research on Public Causes of the Ministry of Land and Resources of the People’s Republic of China (Grant No. 201311015), the Key Project of the National Science & Technology (Grant No. 2016ZX05042-002), the Beijing Higher Education Young Elite Teacher Project and the Fundamental Research Funds for the Central Universities (Grant 2652015331). The authors are grateful to anonymous reviewers and the editor Dr. Giovanni Barla for their careful reviews and detailed comments that helped to substantially improve the manuscript.

References

- Anderson EM (1951) The dynamics of faulting and Dyke formation with application to Britain, 2nd edn. Oliver & Boyd, Edinburgh
- AQSIO, SAC (2009) GB/T 24504–2009 The method of injection/falloff well test for coalbed methane well. Beijing: Standards Press of China, 1–8 (in Chinese with an English abstract)
- Bell JS (2006) In-situ stress and coal bed methane potential in Western Canada. *Bull Can Petrol Geol* 54:197–220
- Bredehoeft JD, Wolf RG, Keys WS, Shutter E (1976) Hydraulic fracturing to determine the regional in situ stress field in the Piceance Basin, Colorado. *Geol Soc Am Bull* 87:250–258
- Brown ET, Hoek E (1978) Trends in relationships between measured in situ stresses and depth. *Int J Rock Mech Geomech Abstr* 15:211–215
- Bustin RM, Cui X, Chikatamarla L (2008) Impacts of volumetric strain on CO₂ sequestration in coals and enhanced CH₄ recovery. *AAPG Bull* 92:15–29
- Cai M, Qiao L, Li C, Ji H, Tan Z, Ren F, Peng H (2010) New development of in situ stress measurement in Chinese mines. In: International symposium on in-situ rock stress, 25–27 August, Beijing, China
- CEA (2000) DB/T 14–2000 Code of hydraulic fracturing and overcoring method for in-situ stress measurement. Beijing: Standards Press of China, 753–766 (in Chinese with an English abstract)
- Chatterjee R, Pal PK (2010) Estimation of stress magnitude and physical properties for coal seam of Rangamati area, Raniganj coalfield, India. *Int J Coal Geol* 81:25–36
- Chen D, Shi JQ, Durucan S, Korre A (2014) Gas and water relative permeability in different coals: model match and new insights. *Int J Coal Geol* 122:37–49
- Chen Y, Tang DZ, Xu H, Li Y, Meng YJ (2015) Structural controls on coalbed methane accumulation and high production models in the eastern margin of Ordos Basin, China. *J Nat Gas Sci Eng* 23:524–537
- Clarkson CR, McGovern JM (2005) Optimization of coalbed-methane-reservoir exploration and development strategies through integration of simulation and economics. *SPE reservoir evaluation and engineering*. December, SPE 88843, pp 502–519
- Connell LD, Lu M, Pan ZJ (2010) An analytical coal permeability model for tri-axial strain and stress conditions. *Int J Coal Geol* 84:103–114
- DB/T 14–2000 (2000) Code of hydraulic fracturing and overcoring method for in situ stress measurement (in Chinese with an English abstract)
- Enever JR, Henning A (1997) The relationship between permeability and effective stress for Australian coal and its implications with respect to coalbed methane exploration and reservoir modelling. In: Proceedings of the 1997 international coalbed methane symposium 1997, pp 13–22

- Enever JR, Casey D, Bocking M (1998) The role of in situ stress in coal bed methane exploration. In: Proceedings of international conference of coal seam gas and oil. Brisbane
- Feng D, Deng HW, Zhou Z, Gao XP, Cui LT (2015) Paleotopographic controls on facies development in various types of braid-delta depositional systems in lacustrine basins in China. *Geosci Frontiers* 6:579–591
- GB/T 24504-2009 (2009) The method of injection/falloff well test for coalbed methane well (**in Chinese with an English abstract**)
- Gentzis T (2009) Stability analysis of horizontal coalbed methane well in the Rocky Mountain Front Ranges of southeast British Columbia, Canada. *Int J Coal Geol* 77:328–337
- Gentzis T (2011a) Stability analysis of a horizontal coalbed methane borehole in the San Juan Basin, USA. *Energy Sources Part A* 33:1969–1984
- Gentzis T (2011b) Stability analysis of two horizontal CBM wells drilled in the deep Mannville coals, Alberta Basin, Canada. *Energy Sources Part A* 33:2281–2290
- Haimson BC (2005) Pre-excavation in situ stress measurements and rational design of coal mines. In: ISRM international symposium—EUROCK 2005, 18–20 May, Brno, Czech Republic
- Haimson BC, Cornet FH (2003) ISRM suggested methods for rock stress estimation-part 3: hydraulic fracturing (HF) and/or hydraulic testing of pre-existing fractures (HTPF). *Int J Rock Mech Min Sci* 40:1011–1020
- Haimson BC, Fairhurst C (1970) In-situ stress determination at great depth by means of hydraulic fracturing. In: Somerton WH (ed) *Rock mechanics—theory and practice*. AIME, New York, pp 559–584
- Hallam SD, Last NC (1991) Geometry of hydraulic fractures from modestly deviated wellbores. *SPE Journal*, SPE 20656
- Han J, Zhang HW, Li S, Song W (2012) The characteristic of in situ stress in outburst area of China. *Saf Sci* 50:878–884
- Hoek E, Brown ET (1980) *Underground excavations in rock*. The Institution of Mining and Metallurgy, London
- Hopkins CW, Frantz JH, Flumerfelt RW, Spivey JP (1998) Pitfalls of injection/falloff testing in coalbed methane reservoirs. In: SPE Permian Basin oil and gas recovery conference. Society of Petroleum Engineers, Midland, Texas, pp 9–24
- Hubbert MK, Willis DG (1957) Mechanics of hydraulic fracturing. *Trans AIME* 210:153–163
- Iannacchione A, Bajpayee T, Prosser L (2007) Methods of determining roof fall risk. In: SME annual meeting, February 25–28, Salt Lake City, Utah (**preprint 07-090, 8**)
- Jeanne P, Rutqvist J, Dobson PF, Garcia J, Walters M, Hartline C, Borgia A (2015) Geomechanical simulation of the stress tensor rotation caused by injection of cold water in a deep geothermal reservoir. *J Geophys Res Solid Earth* 120:8422–8438
- Jiang B, Xu J, Zhu K, Wang J, Wang J, Qu Z (2012) Structural and hydrogeological controls of coalbed methane preservation in the eastern Ordos Basin. *Geol J China Univ* 3:438–446 (**in Chinese with an English abstract**)
- Jie MX (2010) Prospects in coalbed methane gas exploration and production in the eastern Ordos Basin. *Nat Gas Ind* 30:1–6 (**in Chinese with an English abstract**)
- Johnson RC, Flores RM (1998) Developmental geology of coalbed methane from shallow to deep in Rocky Mountain basins and in Cook Inlet-Matanuska basin, Alaska, USA and Canada. *Int J Coal Geol* 35:241–282
- Kang H, Zhang X, Si L (2009) Study on in situ stress distribution law in deep underground coal mining areas. In: ISRM international symposium on rock mechanics—SINOROCK 2009, 19–22 May. The University of Hong Kong, China
- Kang H, Zhang X, Si L, Wu Y, Gao F (2010) In-situ stress measurements and stress distribution characteristics in underground coal mines in China. *Eng Geol* 116:333–345
- Karacan CÖ, Ulery JP, Goodman GVR (2008) A numerical evaluation on the effects of impermeable faults on degasification efficiency and methane emissions during underground coal mining. *Int J Coal Geol* 75:195–203
- Keim SA, Luxbacher KD, Karmis M (2011) A numerical study on optimization of multilateral horizontal wellbore patterns for coalbed methane production in Southern Shanxi Province, China. *Int J Coal Geol* 86:306–317
- Kumar H, Elsworth D, Marone CJ, Mathews JP (2010) Permeability evolution of shale and coal under differential sorption of He, CH₄ and CO₂. In: American Geophysical Union Fall meeting, San Francisco, p 1042
- Kumar H, Elsworth D, Liu J, Pone D, Mathews JP (2012) Optimizing enhanced coalbed methane recovery for unhindered production and CO₂ injectivity. *Int J Greenh Gas Con* 11:86–97
- Li Y, Tang DZ, Xu H, Yu TX (2014) In-situ stress distribution and its implication on coalbed methane development in Liulin area, eastern Ordos basin, China. *J Petrol Sci Eng* 122:488–496
- Li S, Tang DZ, Xu H, Tao S, Shao GL, Ren PF (2015) Evolution of physical difference in various burial depth of coal reservoirs under constraint of stress. *Acta Petrolei Sinica* 36:1–7
- Liu CR (2011) Distribution laws of in situ stress in deep underground coal mines. *Proc Eng* 26:909–917
- Liu QQ, Cheng YP, Yuan L, Tong B, Kong SL, Zhang R (2014) CMM capture engineering challenges and characteristics of in situ stress distribution in deep level of Huainan coalfield. *J Nat Gas Sci Eng* 20:328–336
- Lv YM, Tang DZ, Xu H, Luo HH (2012) Production characteristics and the key factors in high-rank coalbed methane fields: a case study on the Fanzhuang block, Southern Qinshui Basin, China. *Int J Coal Geol* 96–97:93–108
- McKee CR, Bumb AC, Koenig RA (1988) Stress dependent permeability and porosity of coal and other geologic formations. *SPE Form Eval* 3:81–91
- Meng ZP, Tian YD, Li GF (2010) Characteristics of in situ stress field in Southern Qinshui Basin and its research significance. *J China Coal Soc* 35:975–981 (**in Chinese with an English abstract**)
- Meng ZP, Zhang JC, Wang R (2011) In-situ stress, pore pressure, and stress-dependent permeability in the southern Qinshui Basin. *Int J Rock Mech Min Sci* 48:122–131
- Meng ZP, Lan Q, Liu CL, Ji YM, Li SN, Zhang XM (2013) In-situ stress and coal reservoir pressure in Southeast margin of Ordos basin and their coupling relations. *J China Coal Soc* 38:122–128 (**in Chinese with an English abstract**)
- Nelson CR (2003) In deep coalbed gas plays in the U.S. Rocky Mountain Region. AAPG Annual Convention and Exhibition, Denver: American Association of Petroleum Geologists, 2003
- Palmer I, Mansoori J (1998) Permeability depends on stress and pore pressure in coalbeds, a new model. *SPE Reserv Eval Eng* 1:539–544
- Pan Z, Connell LD (2012) Modelling permeability for coal reservoirs: a review of analytical models and testing data. *Int J Coal Geol* 92:1–44
- Paul S, Chatterjee R (2011) Determination of in situ stress direction from cleat orientation mapping for coal bed methane exploration in south-eastern part of Jharia coalfield, India. *Int J Coal Geol* 87:87–96
- Ryan B (2003) Cleat development in some British Columbia coals. *Geology fieldwork 2002, Paper 2003-1*, pp 165–183
- Segall P, Fitzgerald SD (1998) A note on induced stress changes in hydrocarbon and geothermal reservoirs. *Tectonophysics* 289:117–128
- Seidle JP, Jeansonne MW, Erickson DJ (1992) Application of matchstick geometry to stress dependent permeability in coals. In: SPE rocky mountain regional meeting, Casper, Wyoming

- Shi JQ, Durucan S (2004) Drawdown induced changes in permeability of coalbeds: a new interpretation of the reservoir response to primary recovery. *Transport Porous Med* 56:1–16
- Singh PK, Singh VK, Rajak PK, Singh MP, Naik AS, Raju SV, Mohanty D (2015) Eocene lignites from Cambay basin, Western India: an excellent source of hydrocarbon. *Geosci Frontiers*. doi:10.1016/j.gsf.2015.08.001
- Somerton WH, Soylemezoglu IM, Dudley RC (1975) Effect of stress on permeability of coal. *Int J Rock Mech Geomech Abstr* 12:129–145
- Sparks DP, McLendon TH, Saulsbury JL, Lambert SW (1995) The effects of stress on coalbed reservoir performance, Black Warrior Basin, USA. In: *Proceedings of 1995 SPE annual technology conference and exhibition, Dallas, Paper SPE 30743*
- Su XB, Lin XY, Liu SB, Zhao MJ, Song Y (2005) Geology of coalbed methane reservoirs in the Southeast Qinshui Basin of China. *Int J Coal Geol* 62:197–210
- Talebi MH, Heidari S, Moosavi M, Rahimi M (2014) In situ stress measurements of two hydropower projects in Iran by hydraulic fracturing method. *Arab J Geosci* 8(9):7073–7085
- Tang SH (2001) Probe into the influence factors on permeability of coal reservoir. *China Coal Geol* 13:28–30
- Tang SH, Zhu BC, Yan ZF (2011) Effect of crustal stress on hydraulic fracturing in coalbed methane wells. *J China Coal Soc* 36:65–69 (in Chinese with an English abstract)
- Tang X, Zhang J, Shan Y, Xiong J (2012) Upper Paleozoic coal measures and unconventional natural gas systems of the Ordos Basin, China. *Geosci Front* 3:863–873
- Tonnson RR, Miskimin JL (2010) A conventional look at an unconventional reservoir: coalbed methane production potential in deep environments. In: *AAPG annual convention and exhibition, New Orleans, Louisiana, 11–14 April 2010*
- Wang S, Elsworth D, Liu J (2011) Permeability evolution in fractured coal: the roles of fracture geometry and water-content. *Int J Coal Geol* 87:13–25
- Wang S, Elsworth D, Liu J (2013) Mechanical behavior of methane infiltrated coal: the roles of gas desorption, stress level and loading rate. *Rock Mech Rock Eng* 46:945–958
- White CM, Smith DH, Jones KL, Goodman AL, Jikich SA, LaCount RB, Schroeder KT (2005) Sequestration of carbon dioxide in coal with enhanced coalbed methane recovery a review. *Energy Fuel* 19:659–724
- Xu H, Tang DZ, Liu DM, Tang SH, Yang F, Chen XZ, Deng CM (2012a) Study on coalbed methane accumulation characteristics and favorable areas in the Binchang area, southwestern Ordos Basin, China. *Int J Coal Geol* 95:1–11
- Xu H, Zhang JF, Tang DZ, Li M, Zhang WZ, Lin WJ (2012b) Controlling factors of underpressure reservoirs in the Sulige gas field, Ordos Basin. *Petrol Explor Dev* 39:70–74
- Xu H, Tang DZ, Tang SH, Zhao JL, Meng YJ, Tao S (2014) A dynamic prediction model for gas-water effective permeability based on coalbed methane production data. *Int J Coal Geol* 121:45–52
- Xu H, Tang DZ, Tang SH, Zhang WZ, Meng YJ, Gao LJ, Xie SZ, Zhao JL (2015a) Geologic and hydrological controls on coal reservoir water production in marine coal-bearing strata: a case study of the Carboniferous Taiyuan Formation in the Liulin area, eastern Ordos Basin, China. *Mar Petrol Geol* 59:517–526
- Xu H, Tang DZ, Zhao JL, Tao S, Li S, Fang Y (2015b) Geologic controls of the production of coalbed methane in the Hancheng area, southeastern Ordos Basin. *J Nat Gas Sci Eng* 26:156–162
- Xue C, Chi G, Xue W (2011) Effects of hydrocarbon generation on fluid flow in the Ordos Basin and its relationship to uranium mineralization. *Geosci Front* 2:439–447
- Yang C, Zhang J, Tang X (2013) Microscopic pore types and its impact on the storage and permeability of continental shale gas, Ordos Basin. *Earth Sci Front* 20:240–250
- Yao YB, Liu DM, Tang DZ, Huang WH, Tang SH, Che Y (2008) A comprehensive model for evaluating coalbed methane reservoirs in China. *Acta Geol Sin* 82:1253–1270
- Yao YB, Liu DM, Tang DZ, Tang SH, Che Y, Huang WH (2009) Preliminary evaluation of the coalbed methane production potential and its geological controls in the Weibei Coalfield, Southeastern Ordos Basin, China. *Int J Coal Geol* 78:1–15
- Zhao DA, Chen ZM, Cai XL, Li SY (2007) Analysis of distribution rule of geostress in China. *Chin J Rock Mech Eng* 26:1265–1271 (in Chinese with an English abstract)
- Zhao JL, Tang DZ, Xu H, Meng YJ, Lv YM (2013) A permeability model for undersaturated coalbed methane reservoirs considering the effect of coal matrix shrinkage. *Adv Mater Res* 807–809:2413–2420
- Zhao JL, Tang DZ, Xu H, Meng YJ, Lv YM, Tao S (2014) A dynamic prediction model for gas-water effective permeability in unsaturated coalbed methane reservoirs based on production data. *J Nat Gas Sci Eng* 21:496–506
- Zhao JL, Tang DZ, Xu H, Lv YM, Tao S (2015a) High production indexes and the key factors in coalbed methane production: a case in the Hancheng block, southeastern Ordos basin, China. *J Petrol Sci Eng* 130:55–67
- Zhao JL, Tang DZ, Lin WJ, Xu H, Li Y, Tao S, Lv YM (2015b) Permeability dynamic variation under the action of stress in the medium and high rank coal reservoir. *J Nat Gas Sci Eng* 26:1030–1041
- Zuber MD, Sparks DP, Lee WJ (1990) Design and interpretation of injection/falloff tests for coalbed methane wells. In: *SPE Annual technical conference and exhibition, Society of Petroleum Engineers, New Orleans, pp 425–434*